High Efficiency Electric Generator for Chain-less Bicycle

by

Fernando Álvarez González

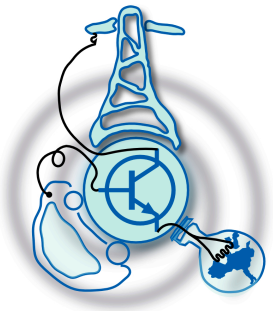

Submitted to the Department of Electrical Engineering, Electronics, Computers and Systems
in partial fulfillment of the requirements for the degree of
Electrical Energy Conversion and Power Systems
at the
UNIVERSIDAD DE OVIEDO
July 2014

Author .....

Certified by .....
Pablo García Fernández
Associate Professor
Thesis Supervisor

Certified by .....
Chris Gerada
Professor
Thesis Supervisor

High Efficiency Electric Generator for Chain-less Bicycle

by

Fernando Álvarez González

Submitted to the Department of Electrical Engineering, Electronics, Computers and Systems
on July 25, 2014, in partial fulfillment of the
requirements for the degree of
Electrical Energy Conversion and Power Systems

Abstract

In this thesis, an electric generator for a chain-less bicycle was designed, optimized and studied in detail. Following a design methodology and employing powerful software tools, the different characteristics were tested through simulation and taken to the limit of its efficiency. Optimization curves were developed for the main parameters and simulation results were provided and studied both analytically and through software analysis. A final satisfactory model was provided and will be manufactured in a near future.

The entire project has been developed within the PEMC (Power Electronics and Machine Control) group at the University of Nottingham.

Thesis Supervisor: Pablo García Fernández
Title: Associate Professor

Thesis Supervisor: Chris Gerada
Title: Professor

Acknowledgments

This project has been entirely developed within the PEMC (Power Electronics and Machine Control) group at the University of Nottingham and it couldn't have been possible without the collaboration of this institution and its members, especially Professor Chris Gerada and research fellow Puvan Arumugam.

Special thanks to all PEMC group members who welcomed me without hesitation and managed to make me feel at home.

Contents

List of Figures

List of Tables

Glossary

SPM	Surface Permanent Magnet
IPM	Interior Permanent Magnet
B	Flux Density
$\mathbf{B}_r$	Remanent Flux Density
λ	Flux Linkage
$\mathbf{H}_c$	Coercivity
μ_r	Magnet Relative Permeability
$\mathbf{L}_g$	Air-gap Length (also g)
$\mathbf{L}_m$	Magnet Length or Thickness
ϕ	Flux
A	Electrical Loading
J	Current Density
f	Frequency
$\mathbf{L}_{stk}$	Stack or Axial Length
$\mathbf{N}_{ph}$	Number of Turns per Phase
m	Number of Phases
p	Number of Pole Pairs
P_a	Air-gap Permeance
P_{sl}	Slot Leakage Permeance
$\mathbf{I}_{rms}$	Effective Value of Current Supply
$\mathbf{A}_{slot}$	Slot Area
$\mathbf{F}_{slot}$	Slot Fill Factor (also K_{fill})
ρ_{cu}	Electrical Resistivity of Copper

Chapter 1

Introduction

Since the invention of electric bicycle in the 1890's the vast majority of progress have due to the evolution of existing batteries, electronics and electric motors technology. Very little has been innovated with regard to the concept of electric bicycle.

The market for electric bicycles is clearly on the rise both in the European Union and beyond its borders. It is a novel alternative that promotes the protection of the environment, the reduction of the carbon footprint, allows riding the bicycle with less effort, making an intelligent management of electrical energy and enabling innovation on their use as a mobile power source. Undoubtedly the evolution of the electric bicycle will continue to create opportunities for development and business.

As it will be extensively presented later in the "state of the art" section, nowadays a great number of electric bicycles are based on the use of batteries to store a limited amount of energy and then either assist a conventional mechanical connection pedaling system or propel the bike for a limited time and distance.

The concept raised here radically changes the way an electric bike is understood. In this system, the mechanical connection is eliminated as seen in figure 1-1 because it has been taken to the limit of its cost-effective efficiency.

Instead, the connection is fully electrically made, the energy obtained from a high-efficiency generator, manage by a power converter and used to power an electric motor that will be the sole mean of propulsion for the bicycle for an unlimited time or distance, as long as the user keeps pedaling. It is then, a pure electric bicycle.

Figure 1-1: Bicycle Concept Example

Through this thesis, the subject of study has been the high-efficiency generator which for obvious reasons accounts for one of the crucial aspects of the system, being the source for all power. The generator type chosen is a permanent magnet one in order to reduce maintenance to the minimum as it avoids the frequent exchange of brushes. Reducing maintenance is another of the crucial aspects which empowers the realization of this project as mechanical transmissions require often a revision or exchange of its pieces.

1.1 Objectives

The objectives of this project are to design a high-efficiency generator that fits the constraints specified in chapter two, to develop and follow a design methodology which allows optimizing the final model and to provide a detailed study of its characteristics.

1.2 State of the art

Although the concept of electric bicycle is not new, nowadays the vast majority of bicycles of this type consist on bulky systems based on the use of batteries. This is in fact nothing but a conventional bicycle with pedal assistance employing batteries and usually a low power electric motor. This vehicles are commonly known as *Pedelec*.

The problem with most current bicycles is that they are transformations of conventional ones with the addition of some electric systems, which is usually known as hybrid-electric bicycles. Examples of this are well known manufacturers on the field such as "LaFree", "Panasonic" or the disappeared "Tidalforce". The proposed system is a full electrical design.

Regarding the legal status of electric bicycles, the European Union directive 2002/24/EC exempts vehicles with the following definition from type approval: "Cycles with pedal assistance which are equipped with an auxiliary electric motor having a maximum continuous rated power of 0.25 kW, of which the output is progressively reduced and finally cut off as the vehicle reaches a speed of 25 km/h (16 mph) or if the cyclist stops pedaling." Based on this definition it is possible to affirm that the proposed system is exempt as the lack of batteries will cause it to stop moving if the cyclist stops pedaling.

Previously, some electric bicycle manufacturers were presented, some others are displayed below:

- AVE Bikes
- Beixo
- BH E-Motion
- BIOBIKE Motorizaciones
- Coluer
- Goes
- Grace Bikes
- Haibike
- Hercules
- Kettler
- Lapìerre
- Legend e-bikes
- Moustache Bikes
- Pedego
- Quipplan
- Wisper
- Yamimoto
- Urban Biker

1.2.1 Generators for electric bicycles

Due to the above specified legal issues most commercial electric bicycles nowadays present brushless motors of 250W but it is not unusual to find power ratings between 120W like "Flebi's Original" and 500W like most heavy or high speed electric bicycles

such as “A2B’s Shima”. One of the most seen companies involved in the electric bicycle motors market is “Bosch”. Its machines are present in several designs from different manufacturers. These bicycles usually employ Lithium-ion batteriesin the range from 24-36V and 8-10Ah.

1.2.2 Chain-less electric bicycles

Nowadays one of the only known commercial electric chain-less bicycle is “Mando’s Footloose” which, although has this revolutionary feature of having no chain, does not get rid of the batteries and has a limited 20-mile operation range. This leaves space in an unexplored market where it is intended to introduce the system under study.

Chapter 2

Generator design

This section presents the first steps taken in the process of designing a generator. The different constraints, topologies and model comparison methodology are introduced in this chapter.

2.1 Constraints

Regarding design constraints, there are mainly three characteristics that were considered as crucial for the correct operation of the machine: Size, torque and voltage. Each of them is presented independently below.

These constraints are a result of previous works regarding a whole electric bicycle focused on mechanical design and power electronics. Size is crucial as it was a result of the mechanical design, in case the outer size differs from the constraints, it would not fit within the frame. Torque is another of the crucial aspects given that it is used to obtain the total output power extracted from the generator and thus present on the whole system, and finally voltage is important due to the power converter stage which requests a certain value and also to avoid as much as possible having to boost up it.

2.1.1 Size

As regards sizing of the machine, the outer measures are provided by the bicycle frame, which given its design, directly assumes a fixed dimensions. The outer diameter of the machine is intended to be 170mm while the axial length is 70mm. The mechanical axle diameter is 25mm.

Taken the above dimensions as the total size of the machine, it is necessary to leave a certain difference for the end turns of the windings and machine housing, the stator diameter selected then is 155mm while the axial length selected is 55mm. The space left for the axle is obviously the same specified before.

2.1.2 Torque

The specified torque expected for the application comes from a study of the performance of different cyclists and their torque generation during operation. From this study is possible to conclude that a right value will be designing the machine for a torque close to 20Nm at a maximum speed of 100rpm.

2.1.3 Voltage

Apropos the voltage, the specifications for the power converters estimate that the DC link will have to count with at least 36V, that is why the machine has been design to provide around 21V of peak voltage per each of the three phases. Calculated as thirty-six divided by square root of three.

2.1.4 Others

Among the difference constraints that affect the design of the generator under study, it could be possible to include others such as speed which has been set to a maximum of 100rpm, value for which the whole system has been calculated. Another indirect constraint variable is price, although it wasn't taken into consideration at first, it was the object of some crucial modification like the final size of the magnets. In

this sense, the machine has been designed paying attention to cost-effective aspects. Finally but not of lesser importance, avoiding saturation has played a relevant role when undertaking upgrades for the final model. The variables that help against the occurrence of saturation have been commented on chapter three.

2.2 Initial model search

In order to obtain a valid design model, the first step consists on providing an initial case which, fulfilling constraints, serves as starting point for the design process. For this purpose, different software tools, presented in detailed through design methodology's section, have been employed in order to compare between several topologies or configuration and choose.

2.2.1 Topologies comparison

While the initial thought was to design directly a surface mounted permanent magnet(SPM) generator, once started the process of selecting an initial model, it was seen as useful to establish a shallow comparison with a topology of magnets located inside the rotor, more specifically an inset permanent magnet generator.

Inset machines weren't studied in detail as the main objective was to compare certain features. It is possible to conclude that although this type of machine require less number of turns allowing saving material they are better configured for higher speeds than that of the application declared on the last section of constraints.

An example of possible configuration for this type of machine is presented in figure 2-1, which presents an inset 24/20 slot/pole configuration.

If compared to a surface permanent magnet generator, it is possible to notice also that the complexity of the first one is greater which may come as another reason for not selecting it. Also with the data obtained from simulation it would be possible to affirm that at the current speed of operation, the efficiency for the surface machine will be bigger. In order to visually allow that comparison declared previously, in figure 2-2 it is possible to see the aspect that the final chosen model (also a 24/20

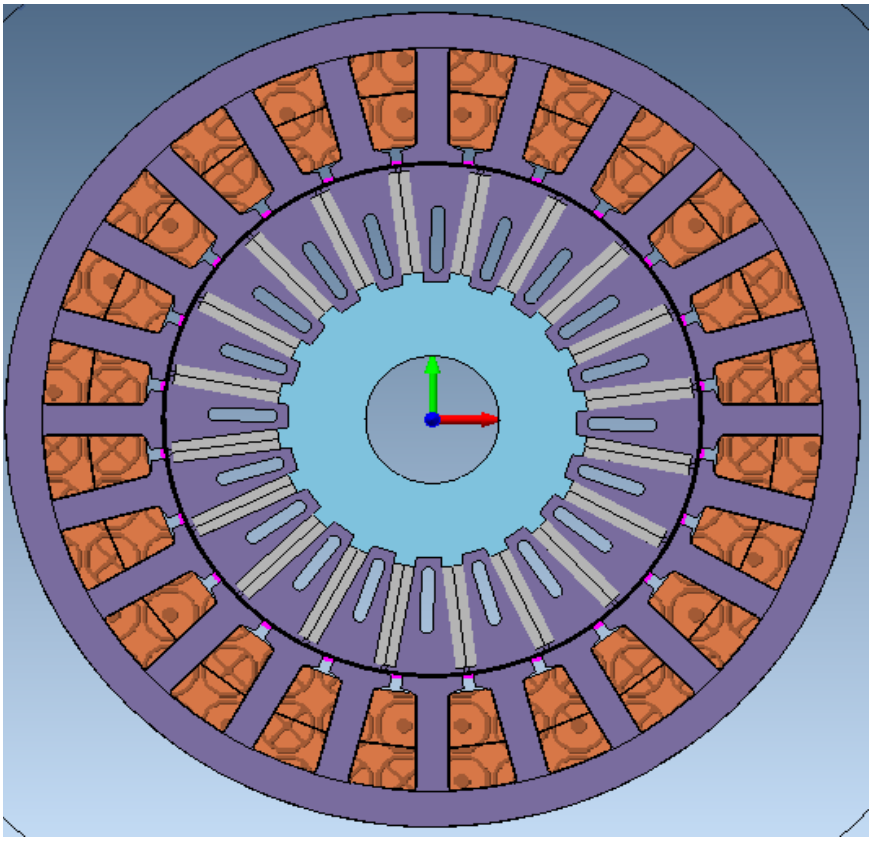

Figure 2-1: Inset Permanent Magnet Generator Example

slot/pole combination) presents.

2.2.2 Configuration comparison

By configuration, the referred design variable is the number of slots and poles, usually known as slot/pole combination. The number of slots and poles has a crucial importance in a motor or generator. It is well known that for low speed applications the number of slots and poles tends to increase as it may be seen on the bigger type of wind turbines been installed offshore in recent years. One reason for this is the possibility of generating a more constant supply of torque and thus power while maintaining low speed values. For high speed systems it is not necessary to include a huge number of slots and poles as the interruptibility will be compensated by the rapid rotation.

Initial models at the beginning of this project development presented a configu-

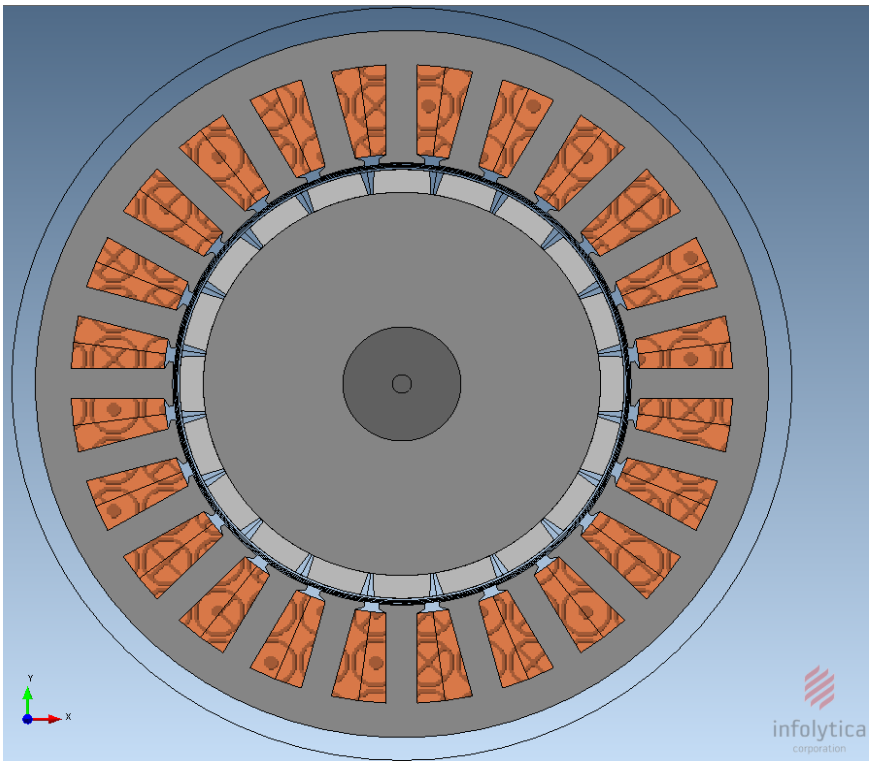

Figure 2-2: Surface Permanent Magnet Generator Example

ration of 12/10 slot/pole combination, as this is a very well tested and very usual configuration which has been proven to work over the years. For many cases the obtained models were proven to present a very good behavior, satisfying design constraints and proving successful when looking at its results. In fact, this configuration could be satisfactory for the case under study as well. The reason why it wasn't chosen at the end is because as the maximum speed is 100rpm, truly, operation speed will tend to be lower, in which case a machine with a higher number of slots and poles will remain valid while the behavior of this one will, at some point, start decaying much faster. In other terms there wouldn't be much difference as well, for instance for price as the size and the amount of conducting material would be necessarily maintained.

Apart from 12/10 and 24/20, which was presented on previous section, another extremely similar configuration was compared, 24 slots and 22 poles. The reason for comparing these three is not arbitrary as they all present good characteristics for low speed as good winding factor and good pull-out torque [1]. Also the three are diametrically symmetric which contrary to non-symmetric machines, increases

bearing life and reduces acoustic noise and vibration. Finally, 24/20 was chosen over 24/22 for being considered as a slightly safer machine in terms of control and recommended by advice of one of the project supervisors. In fact there is controversy about which machine presents better characteristics.

Finally it is important to point out that at a very early stage of this project, a vast number of slot/pole configurations were rejected for having variables far worse than the one presented above. Among them there were the following:

- 12 slots / 14 poles
- 15 slots / 10 poles
- 15 slots / 14 poles
- 18 slots / 10 poles
- 24 slots / 28 poles
- 30 slots / 28 poles

2.2.3 Initial values

Initial values for most characteristics were obtained in most cases employing one of the software tools which will be presented in following sections and then compared to the values obtained through expressions in order to test its validity.

For instance, although it is possible to obtain the number of turns through various expressions, it is much faster to provide an estimated value, simulate the system and from there calculate in what measure will the obtained torque or voltage seem reduce in relation with that value.

Once the results are approximated, it is easy to provide initial design variables such as the current supply been given that in order to maintain the torque constant, the result of multiplying number of turns and supply current must be maintained. In this way, once the torque is at a valid point, lets say 20 newton-meter, the number of turns and supply current can be modified to reduce losses, increase voltage or others by for instance reducing that current and increasing the number of turns.

In this way, giving general initial values like a number of turns equal to 44, a supply current equal to 10 amperes, a magnet thickness or height equal to 6 millimeters it is possible to rapidly obtain and initial model which would, following a design

methodology, allow a further optimization with the consequent obtainment of a final satisfactory model.

Windings

Winding type chosen is a two layer side-by-side one. Initially, the type over-under was tested but rapidly discarded as it was proven that would lead to a less efficient winding.

The winding process has been carried out by comparing the windings automatically generated by one of the software tools, *MotorSolve* with the examples provided at the end of reference [3].

Phase A		Phase B		Phase C	
In	Out	In	Out	In	Out
1	2	9	10	17	18
6	7	14	15	22	23
8	7	16	15	24	23
13	12	21	20	5	4
13	14	21	22	5	6
18	19	2	3	10	11
20	19	4	3	12	11
1	24	9	8	17	16

Table 2.1: Windings Table

Once a configuration has been chosen it is performed according to table 2.1 which indicates the starting and ending point of each winding, this is, the coil goes from *in* to *out* repeatedly until the whole phase is formed. The numbers in the table refer to the slots which go from 1 to 24 starting from the slot on the right hand part of the model, just above the imaginary line that would divided the machine horizontally in two. *PhaseA* winding can bee seen selected on figure 2-3.

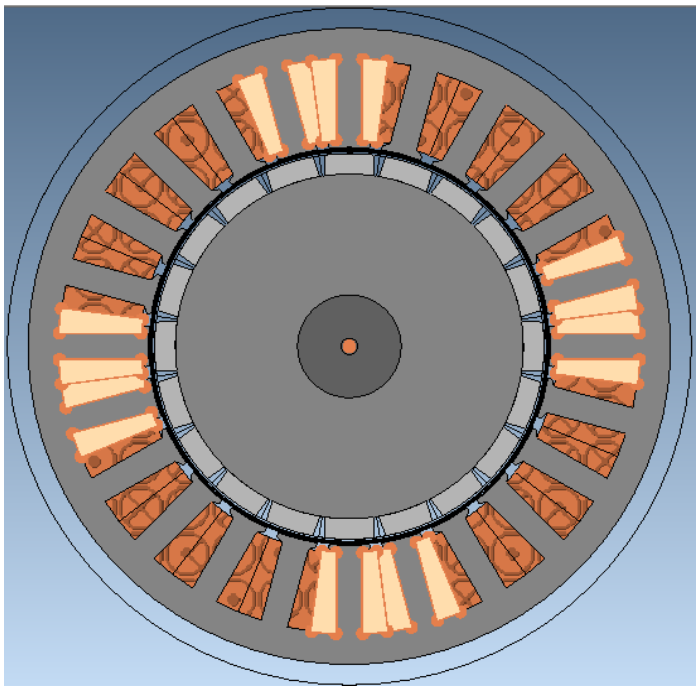

Figure 2-3: MagNet Software Winding Phase A

Materials

Regarding materials employed for simulation, four different ones were used for all parts fo the models. Stator and rotor yokes are made of "non-oriented EN10106 fully processed silicon steel", more specifically $M250-35A$ which main characteristics are a lamination thickness of $0.35mm$ mass density of 7600kg/m^3, a specific heat of 490J/(kg°C) and a thermal conductivity of 25W/(m°C). The gaps between layers of this material are usually filled with epoxy resin.

The shaft is made of non-magnetic stainless steal "304" which main characteristics are a lamination thickness of $0.35mm$ mass density of 8190kg/m^3, a specific heat of 500J/(kg°C) and a thermal conductivity of 16.2W/(m°C).

The magnets are made of neodymium iron boron "48/11" which is one of the combinations with a highest remanent flux density and good enough thermal behavior.

Finally, the conductive material employed for the software model is "Copper: 100%IACS". Although generator's housing has not been taken into account for MagNet simulation, a possible material for it could be "CR 10: Cold rolled 1010 Steel".

2.3 Design methodology

During the development of this project, a design methodology was applied in order to arrive at the solution design in the shortest possible time. The process followed consisted on first, familiarizing with the concepts which were mostly new for reasons of previous author's background. Secondly, taking into account size design constraints, an initial and not very accurate model was provided, allowing to apply the primary aspect of this methodology, which has been model optimization. Finally, once the model was optimized, a detailed study was perform in order to study the obtained results and to provide the project with a deeper and more scientific compound.

2.3.1 Software tools

In order to fulfill the design methodology, software tools played a crucial role, allowing the basics for this project which are simulation and results post-processing. Among the tools employed three stand for their importance: $MotorSolve$, $MagNet$ and $MATLAB$.

MATLAB

Been $MATLAB$ a very well known software tool, a wide explanation of its capabilities is not necessary. $MATLAB$ was employed mainly for two different purposes. The first one was to serve as a script shooter which put together different $VisualBasic$ codes that allow one of the other two tools, $MagNet$, to automatically generate and simulate a model based on an already defined variables.

The other purpose for the employment of $MATLAB$ was the post-processing of the results obtained when simulating with the other two softwares employed.

Motor Solve

$MotorSolve$ is one of $Infolytica$'s software tools which allows rapidly defining, generating and simulating a motor or generator model. This tool is quite useful for

obtaining an estimated idea of a certain configuration or topology. For this reason it was crucial at an early stage of this project.

The best about this software is that been a very intuitive and easy tool to employ it is possible to create a model stipulating a few constraints, generating $MotorSolve$ values for the pending elements. Also, once the model has been generated and after any number of simulations have been performed, it is possible to modify any variable.

The main drawback about it is that when compared with $MagNet$, another $Infolytica$'s software tool, its results are generally not trusted as totally accurate. Also, modifying one variable may end up with the automatic correction of several other ones.

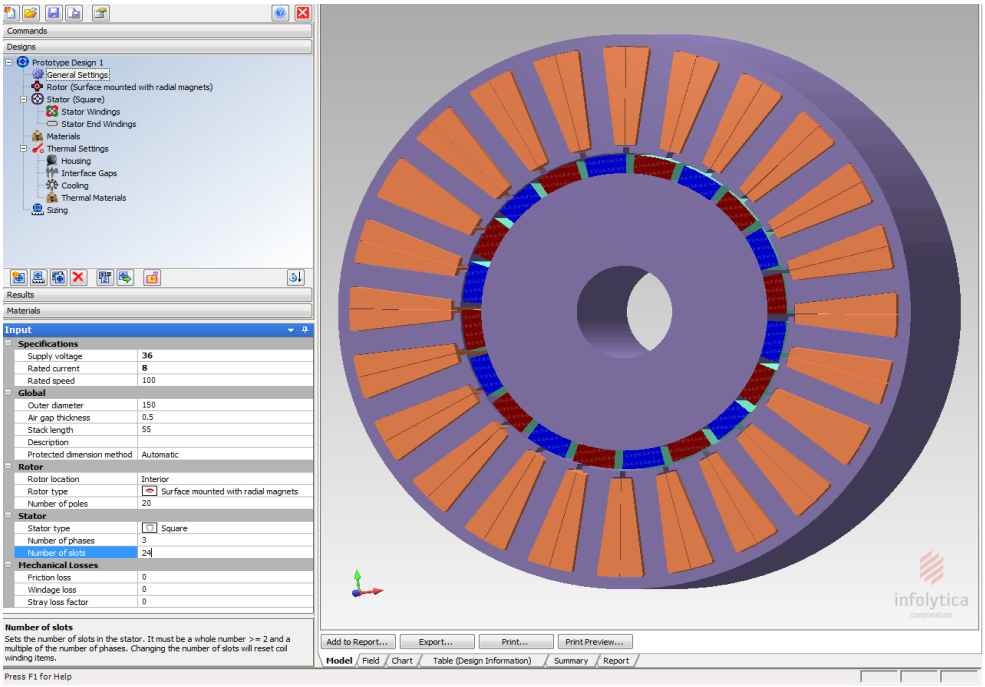

Figure 2-4: Motor Solve Software Tool Example

$MotorSolve$ presents itself a good display of values allowing study its simulation results without necessarily needing another tool as $MATLAB$. An example of the aspect that $MotorSolve$ presents has been shown in figure 2-4. The aspect that the results present when provided directly by $MotorSolve$ in graphic form after a motion analysis simulation are also presented in figure 2-5.

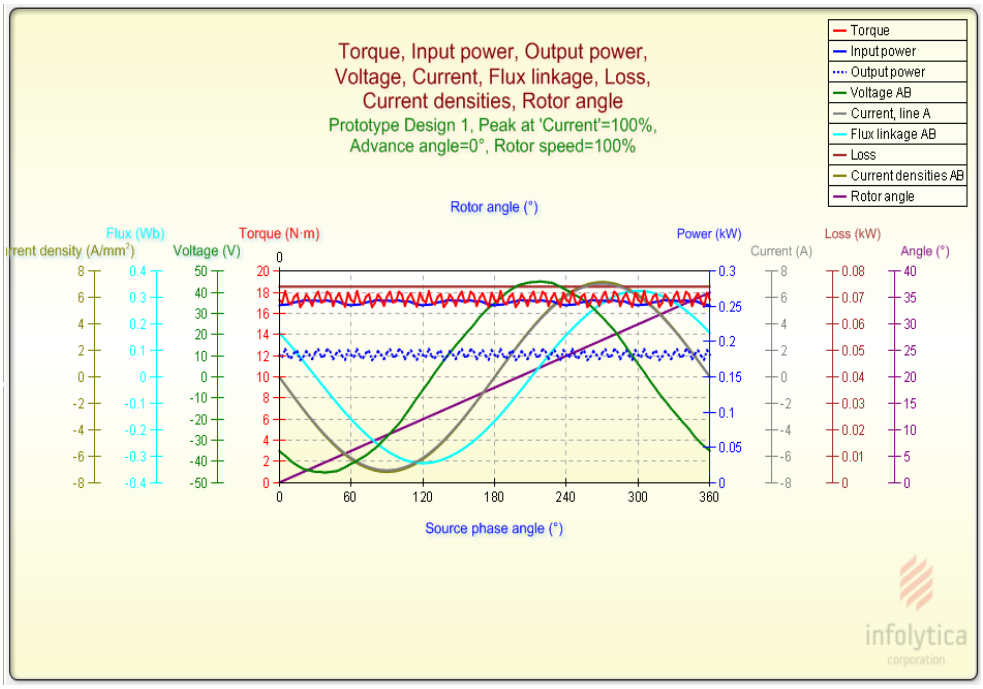

Figure 2-5: Motor Solve Software Tool Results

MagNet

MagNet is the main tool employed for fulfilling the objectives of this project. It is a well trusted powerful finite element software that allows obtaining very accurate results with the possibility of generating the models through script, allowing a rapid generation, simulation and post-processing of models.

The main drawback of this software is that once the model has been built, it is not easy to modify one variable, in fact, when working through script it is usually easier to generate a whole new model.

As it does *MotorSolve*, *MagNet* also presents a numeric results displaying window but it is usually needed to perform a post-processing in order to obtain average values or reorganize the values. On the other hand, it also allows looking at several parameters directly displayed on the model surface such as flux lines or flux density as it is shown inf figure 2-6.

In order to have an average idea of the finite element division or *mesh* developed by the software, figure 2-7 provides a glimpse of it, on which on the only information needed from the user is the division size, in the scale under use (millimeters for the

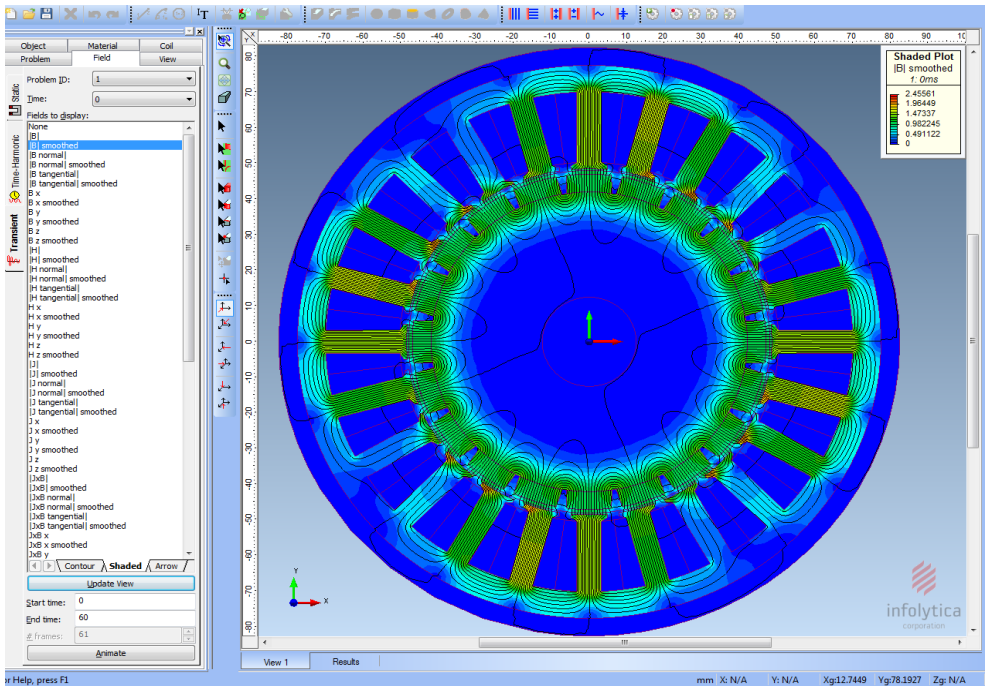

Figure 2-6: MagNet Software Tool Flux Results

case under study), for each part.

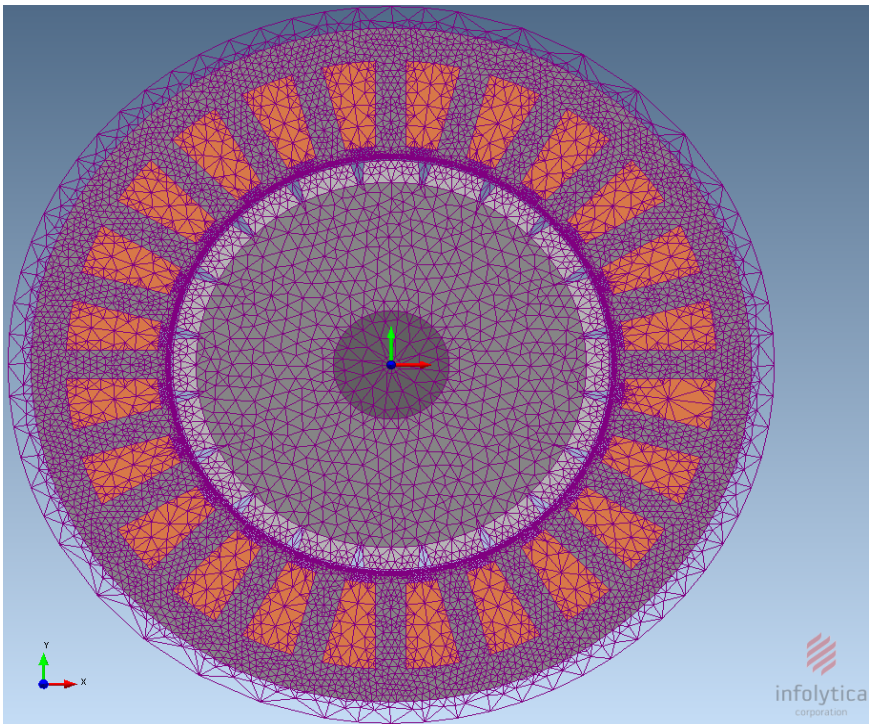

Figure 2-7: MagNet Software Finite Element Mesh

Chapter 3

Model optimization

In order to achieve satisfactory features that meet the needs of design, a model optimization process has been pursued divided mainly into two well differentiated stages, mayor changes affecting vital elements in the generator such as the magnet thickness or the rotor diameter and parametric changes that affect minor features used to perform a finer adjust of the system.

3.1 Major parameter changes

Among the mayor parameter changes it is possible to find the number of turns, supply current, magnet thickness and span angle, tooth width ratio or rotor diameter.

3.1.1 Number of turns and supply current

The two parameters displayed on the title of this section are put together as their values are intrinsically linked, this is, the parameter taken into account for the design was the product of these two. In this sense, every time one of the two values was modified, the product of both variables was kept constant by increasing the other one in accordance.

The reason for modifying one or the other could for instance the look for a higher value of voltage in which case, in order to maintain the torque constant, the number

of turns would increased while the current would decreased.

It is important also to keep in mind that changing mayor variables would affect crucial aspects such as the efficiency, been calculated employing the losses and thus, copper losses, which are dependent in greater way of the current than in the number of turns. This dependence can be easily explained employing a simple expression to define power.

$$P = RI^2 \tag{3.1}$$

It is easy to imagine that if the number of turns increases, copper losses will increased as well but as the current value is squared its effect will have a higher impact.

Taking all of this into account the number of turns and current supply were chosen in order to fulfill the torque and voltage constraints at the same time that keeping the efficiency as high as possible.

Taking as initial values those indicated in the previous section, this is, a current value of 10A and a number of turns equal to 44, we have followed a process of creation of new models and simulation to obtain the desired values. Since any small change in the system can lead to unfavorable results during this process the other variables have been kept constant. The results used to study the effect of changing these two values were torque, voltage and efficiency.

The final values chosen were a supply current of 8A and a number of turns equal to 40. The final values for the three crucial results were an efficiency slightly higher than 88 percent, a torque value of 19Nm and a voltage of 21V. But, as nine variables and not two were taken into account, it is necessary to present the effect of the pending ones.

3.1.2 Magnet thickness

When facing magnet size, two variables are taking into account, the first one, thickness, is the one treated in this section, the second is magnet angle or span which is seen later.

To achieve a satisfactory value of magnet thickness, its effect has been studied

following the design methodology employed for most of the variables. It is easy to come to the conclusion that up to a reasonable value, the bigger the magnet, the better the results. This is true, in fact the best results were achieved for a value of 11mm magnet thickness but there is a there is an important reason that advises against using that size, price.

Given that magnetic materials are usually the most expensive part of the machine, a new value of 5mm is proposed taking into account a huge change on price but a minor one in results. Again, there wouldn't be much difference between selecting 5mm or a value a bit lower but the chosen one complies well enough with the cost-effective aspect.

Paying attention to figures 3-1, 3-2 and 3-3, it is possible to see that efficiency, torque and voltage are at its highest point at the value of 11mm indicated before but it is also easily seen than the values vary between relatively similar values.

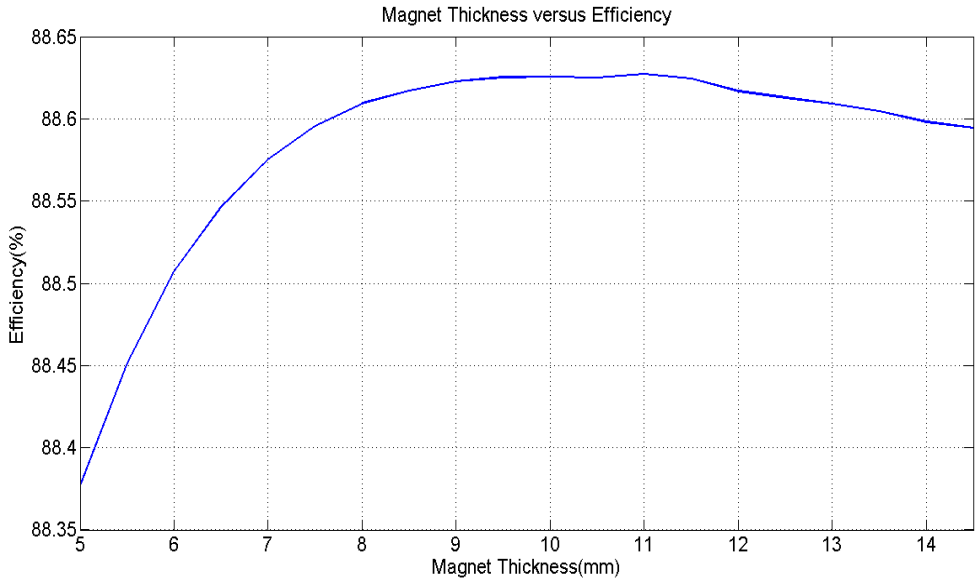

Figure 3-1: Magnet Thickness versus Efficiency

Another factor that advices against selecting a bigger value of magnet thickness is the possible magnetic saturation present on the stator teeth.

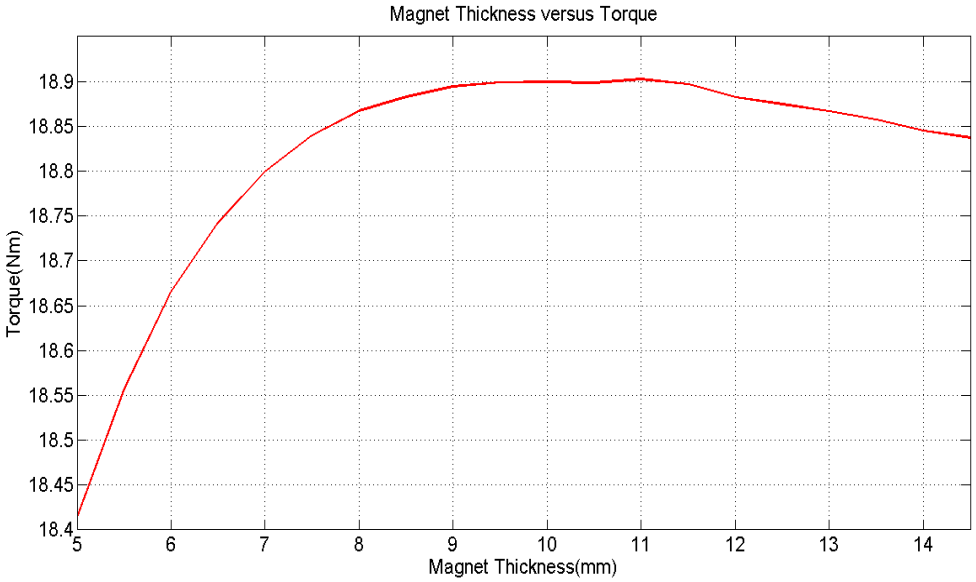

Figure 3-2: Magnet Thickness versus Torque

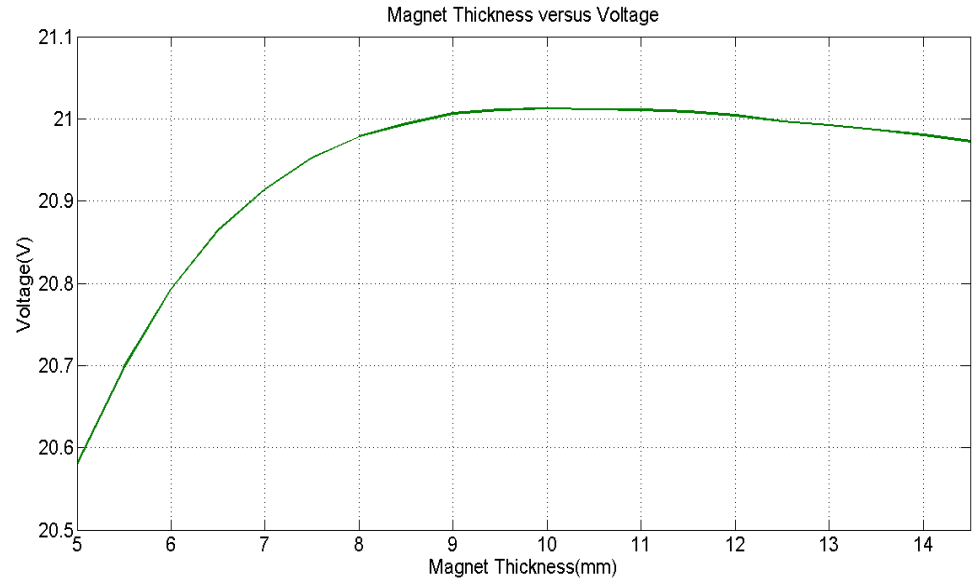

Figure 3-3: Magnet Thickness versus Voltage

3.1.3 Magnet angle

When talking about magnet angle the referred variable can be considered the width but taking into account that the magnet is located on top of a the rotor surface it is more convenient to talk about angle.

The value chosen for this variable is based on similar premises than the previous

one but in this case saturation comes as even more important than price as it is necessary to avoid the presence of flux lines "jumping" between poles.

From the initial value presented in chapter 3, only few modifications have been needed to select the final one. Been 15 degrees the initial one for the topology and slot/pole combination under study, 16.5 degrees is the final one. The reason is simply that above that value flux lines incur in behaviors not wanted due to the increased proximity between poles.

It is possible to affirm that the bigger the magnets, the better the results within the range previously described.

3.1.4 Rotor diameter

Given as constraint the outer stator diameter, the value of the inner and thus rotor diameter is another variable that must be set. Rotor diameter has been selected in order to maximize the resulting torque. It has been obtained as most suitable a value of 95mm.

As in most cases and most engineering problems the selection of rotor diameter is an exchange that must be balanced, this is, if increased a lot, it would reduce the slot area incurring in possible constraints to the amount of copper conductors which affects mainly the generated voltage. In case of decreasing it too much, torque will be dramatically reduced.

3.1.5 Tooth Width Ratio

Tooth width ratio is a characteristic that express the width of the slot teeth with a value varying from 0 to 1. In reality 0 and 1 are never going to be acceptable values and real applications will be usually in the range from 0.5 to 0.7.

The main effect of the modification of this variable is the increase or reduction of the amount of copper conductor as seen on figures 3-4 and 3-5, for this reason, the smaller the value, the higher the torque and the voltage while, the bigger it is set, the better the efficiency will be as a reaction of reducing the amount of copper and

thus the its main source of losses.

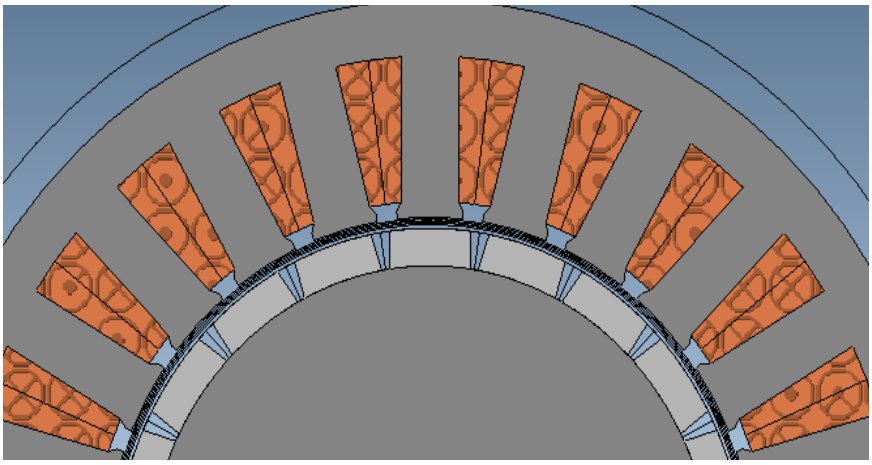

Figure 3-4: Tooth Width Ratio equal to 0.5

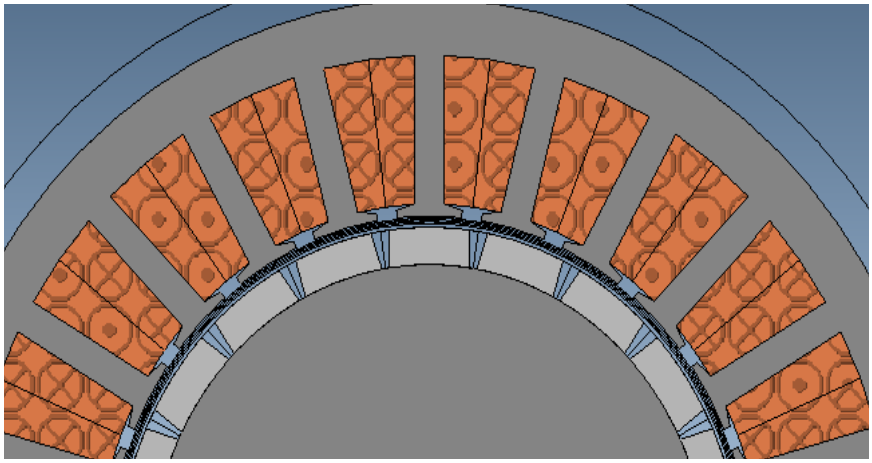

Figure 3-5: Tooth Width Ratio equal to 0.7

As it was done for most characteristics, the values were modified and tested for ten different cases from 0.5 to 0.725 in steps of 0.25. This study pointed out that a satisfying value could be 0.6 which is the one chosen for the final model. The graphs summarizing the effect of this changes has been displayed on figures 3-6 and 3-7.

Perhaps this variable stands for the obvious opposition in their graphs where it can be seen how choosing between one value or another should be taken based on an election that compromises one of the results. For the case under study, it has been decided to promote often and up to a maximum value of 20Nm, the torque.

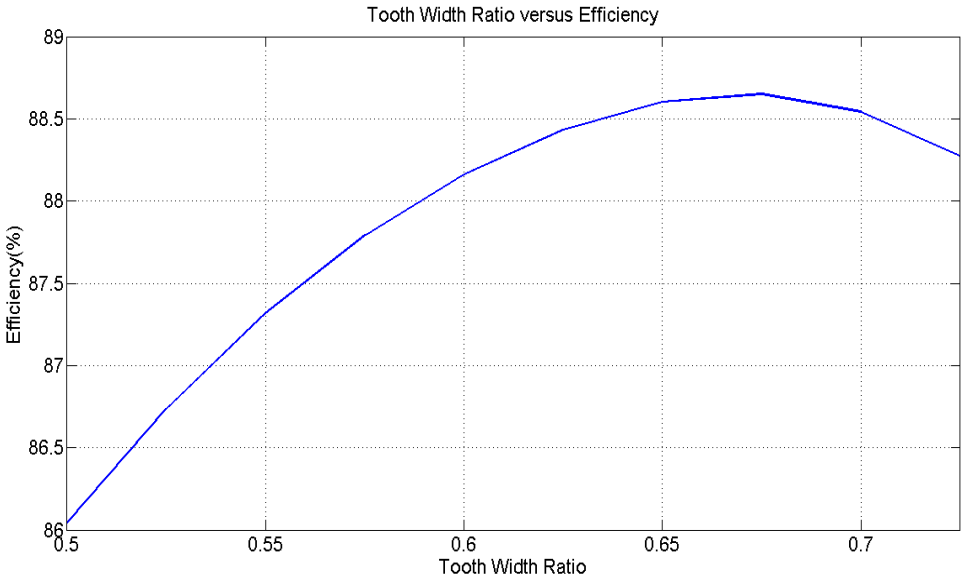

Figure 3-6: Tooth Width Ratio versus Efficiency

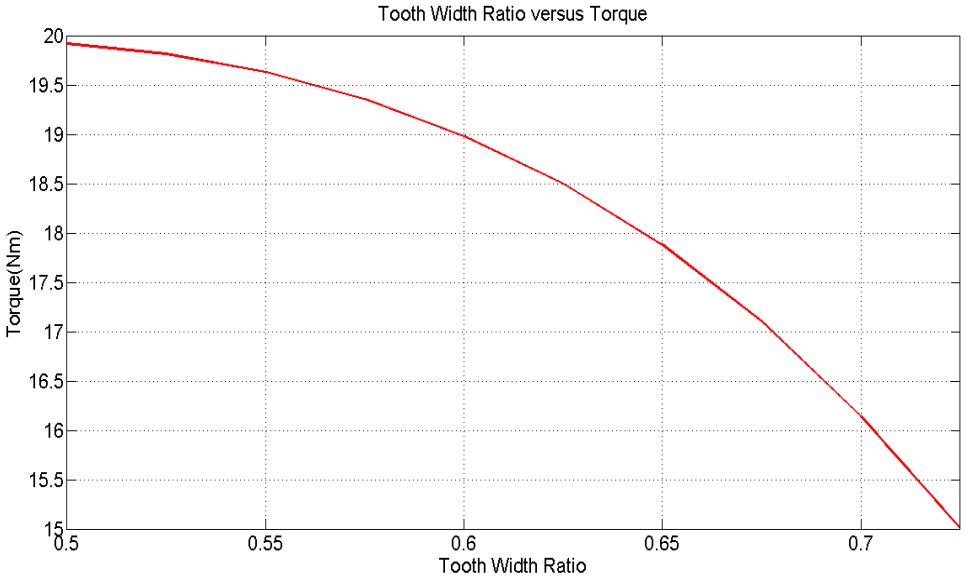

Figure 3-7: Tooth Width Ratio versus Torque

3.2 Parametric changes

By parametric changes the variables referred to are those that affect the design results in a minor way. Among these variables it is possible to find slot opening, slot wedge angle or tooth tip height.

3.2.1 Slot opening

Slot opening is the name usually employed to define the separation between the tooth tips of each slot. Its effect has been studied as it was done before for magnet thickness by modifying the variable subsequently and gathering the values in the graphs displayed on figures 3-8 and 3-9.

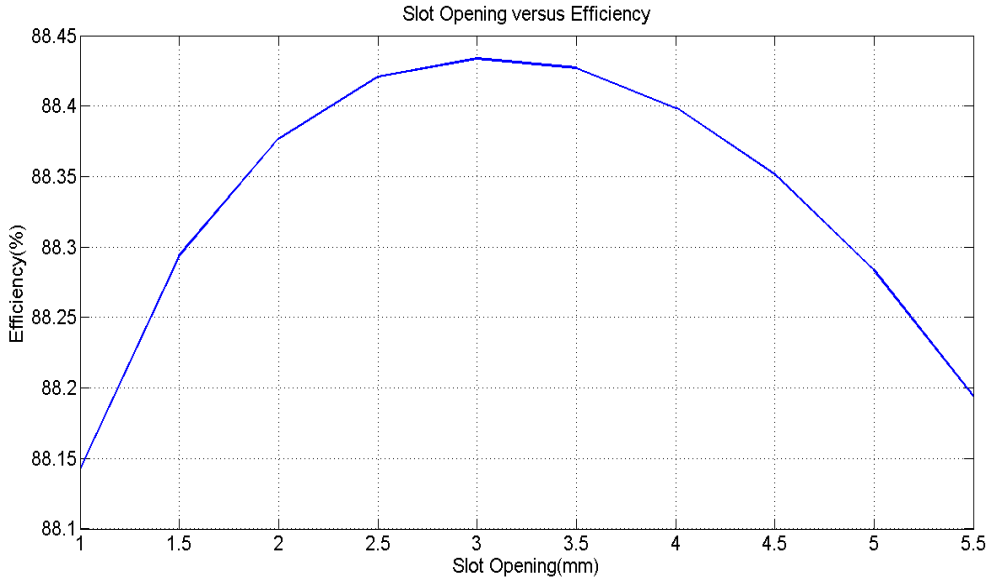

Figure 3-8: Slot Opening versus Efficiency

Figure 3-8 shows how the efficiency is affected by the modification of this value while figure 3-9 shows the effect on the torque. If paying attention, it is possible to see that both graphs have an almost exact response when increasing the value from 1 to 5.5mm.

The effect of the slot opening configuration may be seen in a more visual approach in figures 3-10 and 3-11. In these figures it is easily seen this variable affects the teeth's shape. It has been seen how the relation between slot opening and efficiency or torque is quite similar, on the other hand, the relation between slot opening and voltage presents a totally different shape as it may be seen on figure 3-12.

It is possible to affirm that the best values for both efficiency and torque are those generated when choosing a 3mm slot opening.

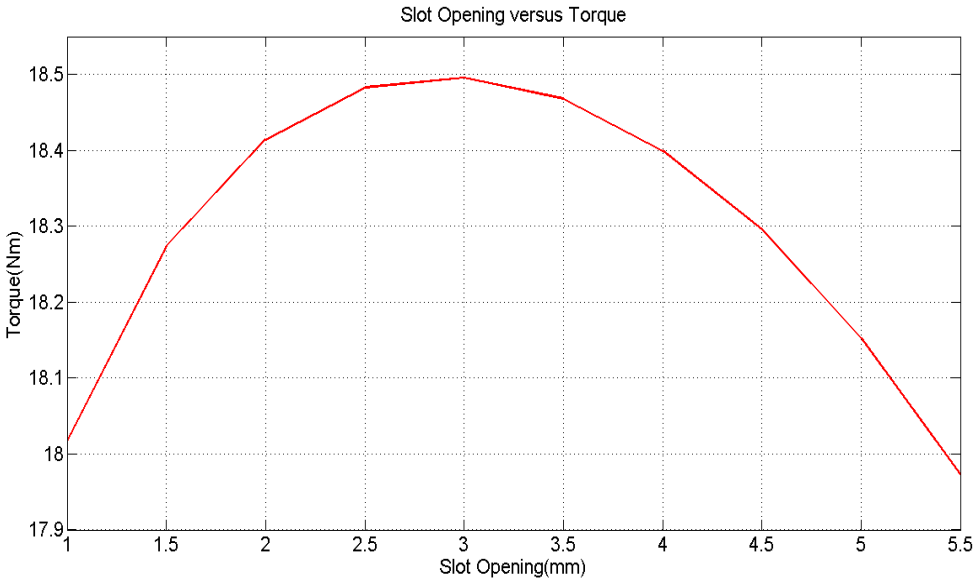

Figure 3-9: Slot Opening versus Torque

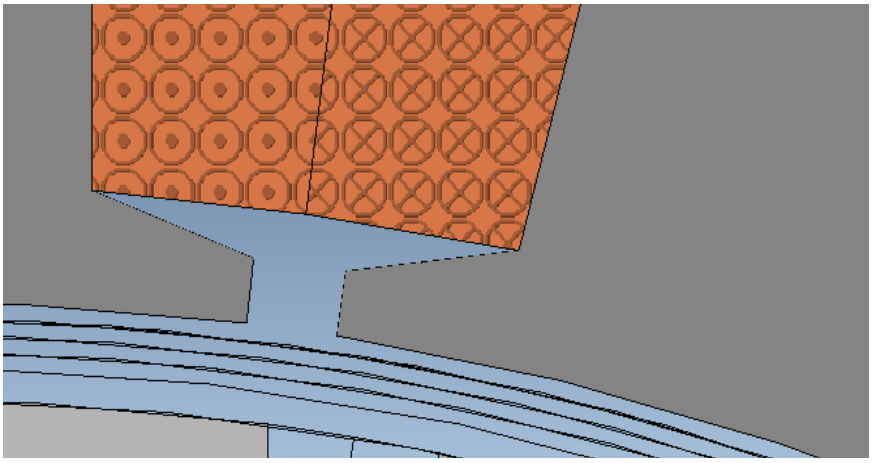

Figure 3-10: Slot Opening equal to 0.5

3.2.2 Slot wedge angle

Slot wedge angle is a variable that affects visibly the shape of the stator teeth. In order to illustrate this, figures 3-13 and 3-14 show the huge visual difference that changing this characteristic may have on the model.

The effect on the results is not so drastic for the range studied, beginning with an angle of zero degrees and up to forty-five the difference in efficiency is less than one percent and in torque less than 0.2Nm. It has a noticeable effect in voltage though,

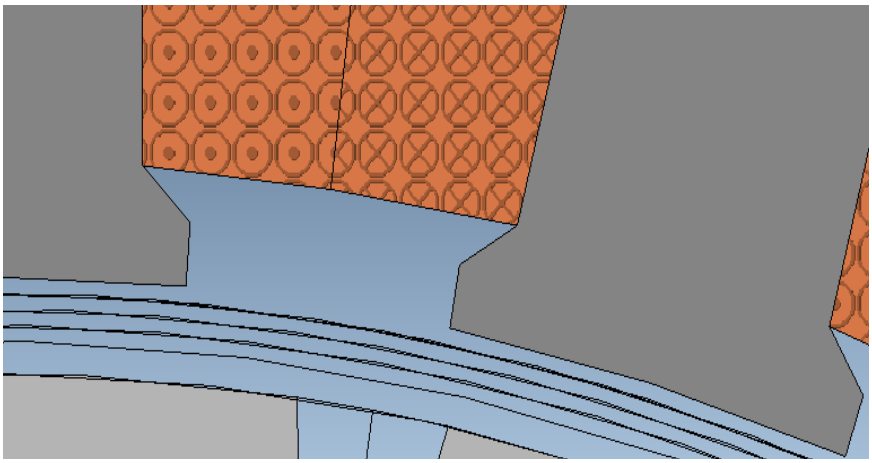

Figure 3-11: Slot Opening equal to 5

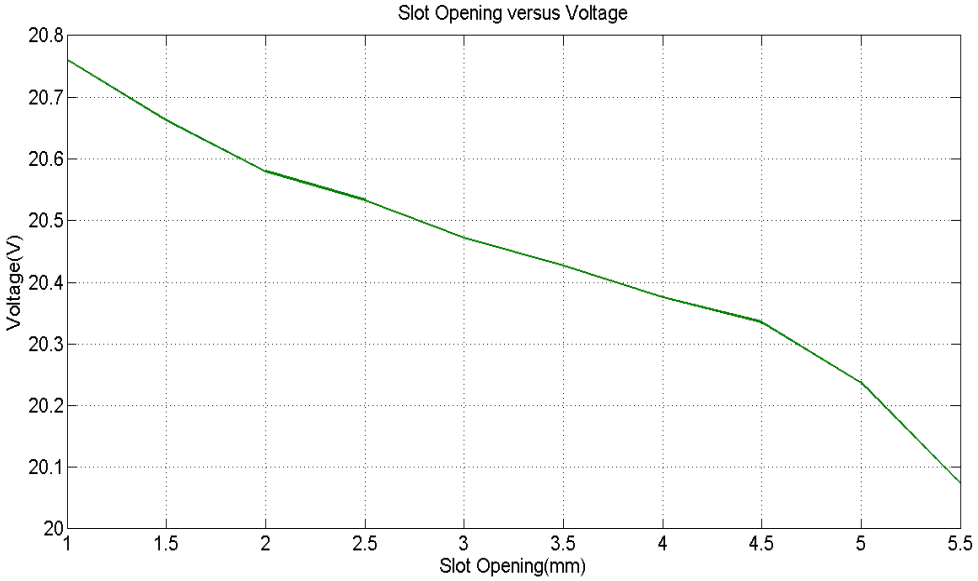

Figure 3-12: Slot Opening versus Voltage

varying from 19.3V to 21.5V. The reason for this change in voltage is that, as it may be seen, the amount of copper conductor is being limited by this change.

As it was done before, the graphs representing this changes are included in 3-15 and 3-16, and similarly to what was seen for tooth width ratio, the graphs oppose to each other so the choice is made in order to promote the highest value of torque or at least as high as possible without compromising the efficiency in excess.

Although for the final value both 15 and 20 degrees would be acceptable values, finally a value of 15 has been chosen as in that range the torque does not vary much

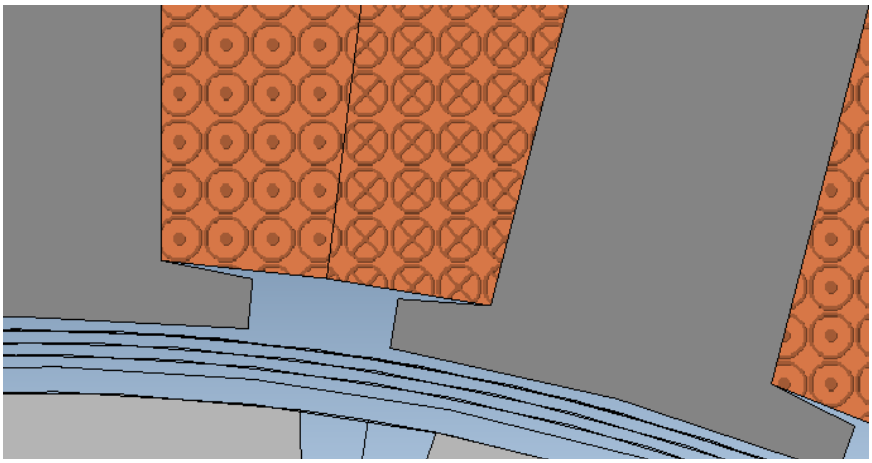

Figure 3-13: Slot wedge angle equal to 5

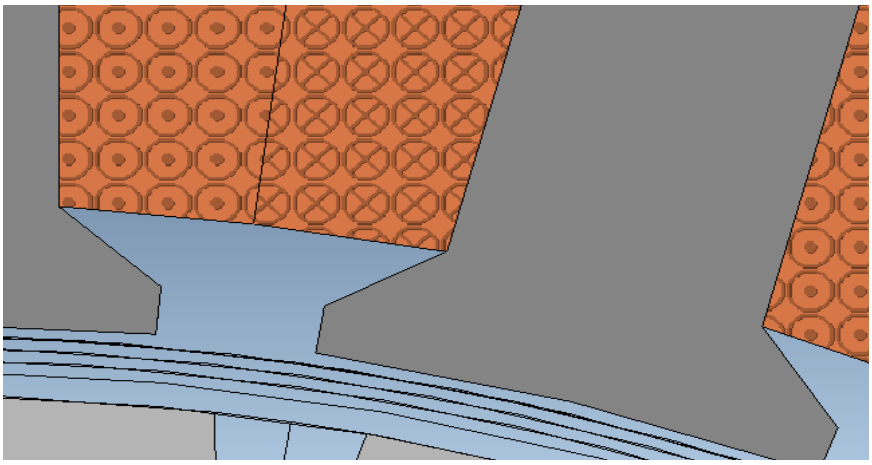

Figure 3-14: Slot wedge angle equal to 35

but the efficiency does.

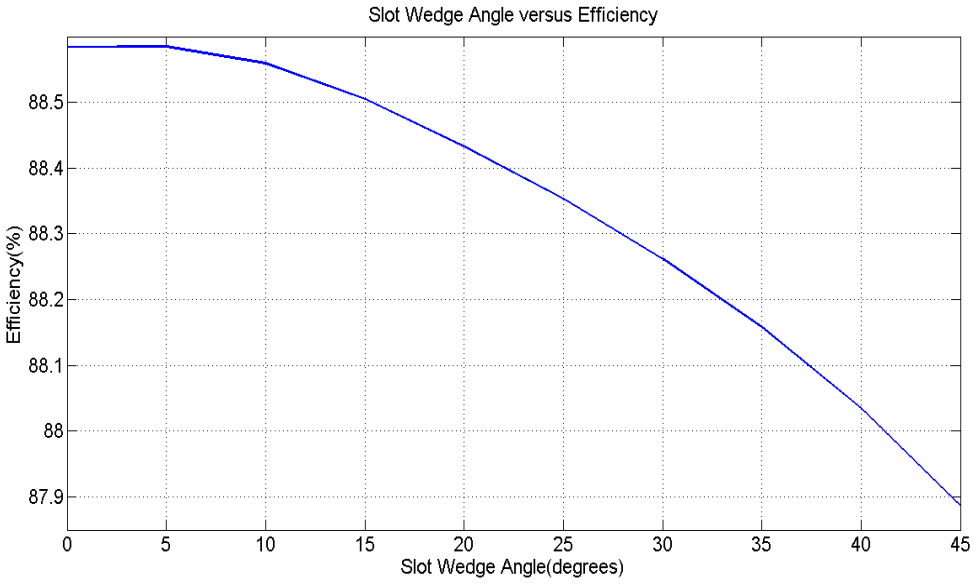

Figure 3-15: Slot Wedge Angle versus Efficiency

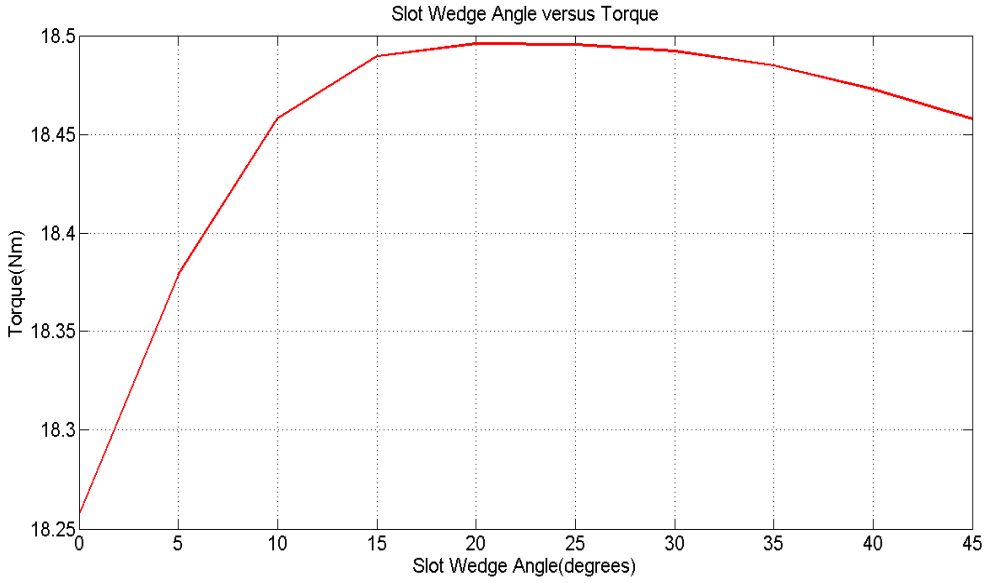

Figure 3-16: Slot Wedge Angle versus Torque

3.2.3 Tooth tip height

The variable usually known as tooth tip height hasn't been studied in detailed as its modification is often employed as a way to avoid saturation on the teeth tips rather than to improve in a visible way the results. If increased, the effect seen on the crucial results is an increase in phase peak voltage but a decreased in torque and efficiency.

Decreasing it under the selected value of 1mm is not a good idea either as it would became a small and fragile edge.

Chapter 4

Characteristics study

This chapter presents the different characteristics of the machine that have been taken into account for detailed study seen their importance for the overall performance during operation.

4.1 Air-gap flux density

Flux density B may be defined as $B = \mu H$ where H is the magnetic field intensity and μ the magnetic permeability. Its unit of measurement is the Tesla(T).

Its behavior can be shown employing the magnetization curve or B-H curve which shows the magnetic saturation of the different materials, this is, the maximum value of B that it is possible to achieve.

Regarding the air-gap length, the $B - H$ curve of a magnetic equivalent circuit is affected by the presence of this air gap in the form that permeability of non-magnetic material is low so greater values of H are required to obtain the same value of B compared to magnetic materials. On the other hand, if no air-gap is present then the slope becomes as steep as possible, and the $B - H$ loop will represent the closest approximation of the characteristic of the magnetic material. In this case it is not easy to select an air gap flux density value towards the practical application (design).

Also, due to the increased reluctance of the air gap, the flux spreads into the surrounding medium causing the apparition of non-desired phenomena such as flux fring-

ing which may end up increasing losses in nearby conductors (eddy current losses).

An example of flux density distribution present on the generator is provided by MagNet and seen on figure 4-1 and, with a closer approach, in figure 4-2.

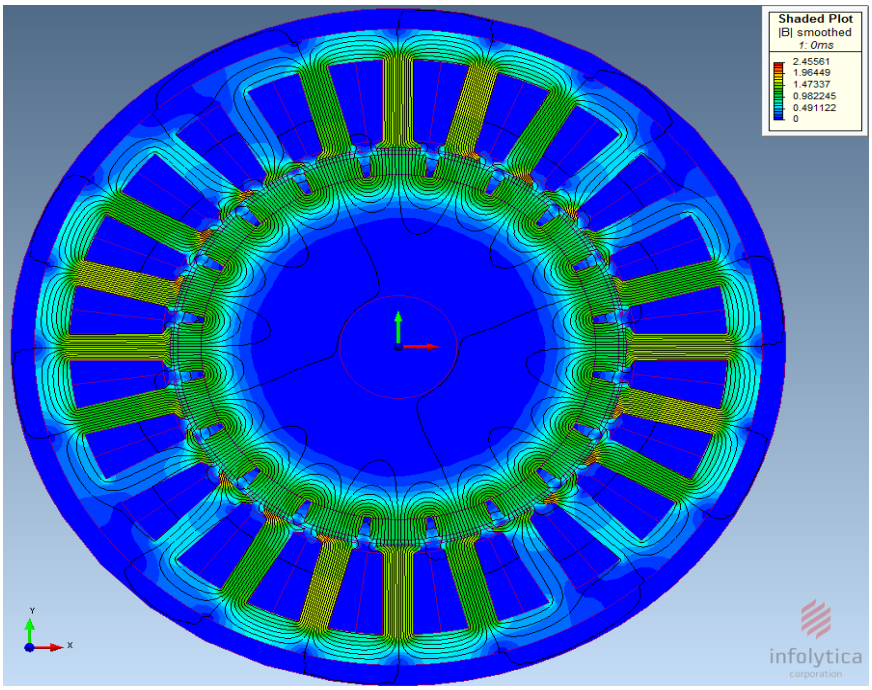

Figure 4-1: Flux Density

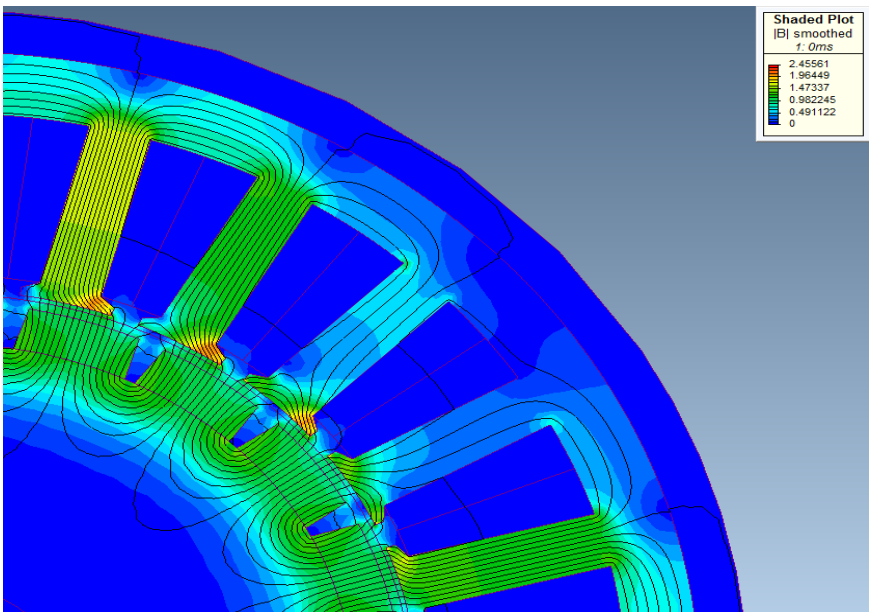

Figure 4-2: Flux Density Detailed

Values presented oscillate between 0T for the darkest blues zones and 2.45T for some small regions which present a slight amount of saturation. The majority of the colors displayed oscillate around 1T.

Air-gap flux density depends on the MMF, the magnetic boundary conditions, the length of the air-gap, the effect of the slot openings and the shape of the pole face. It has two main components, the flux density produced by the stator currents passing through the windings and the rotor magnets flux density.

It is not an easy task to provide an expression that describes precisely the air-gap flux density taking into account both components, that is why usually in order to obtain an approximate value the following equation is employed which takes under consideration only the component due to the permanent magnets in the rotor. A good estimation is a value close to 0.9T obtained employing expression 4.1.

$$B_g = \frac{B_r}{1 + \mu_r \frac{L_g}{L_m}} \tag{4.1}$$

Expression 4.1 perfectly represents the permanent magnet component of the air-gap flux where B_r is the permanent magnet remanent flux equal to 1.1T, μ_r is the magnet relative permeability equal to 1.05, L_g is the air-gap length equal to 1mm and L_m is the magnet length which final chosen value is equal to 5mm.

4.2 Phase flux linkage

Flux linkage is measured in units of weber per turn (Wb/turn) and usually displayed by the symbol λ. In permanent magnet machines, flux linkage has two clearly differentiated components: One due to the permanent magnets remanent flux and the other due to the flux generated when current circulates through the stator windings [2]. While obtaining the values through mathematic expressions is rather complex, getting them employing one of the two software tools described in the design methodology is much easier. The software tool employed is MagNet.

The way to obtain each component of the flux linkage consist on calculating the

value due to the permanent magnets first, and then subtract it from the total. For this purpose, a no-load test has been performed by setting to zero amperes the current sources employed for simulation. The result of doing this has been displayed in figure 4-3, having a maximum value of 0.1702 Wb/turn.

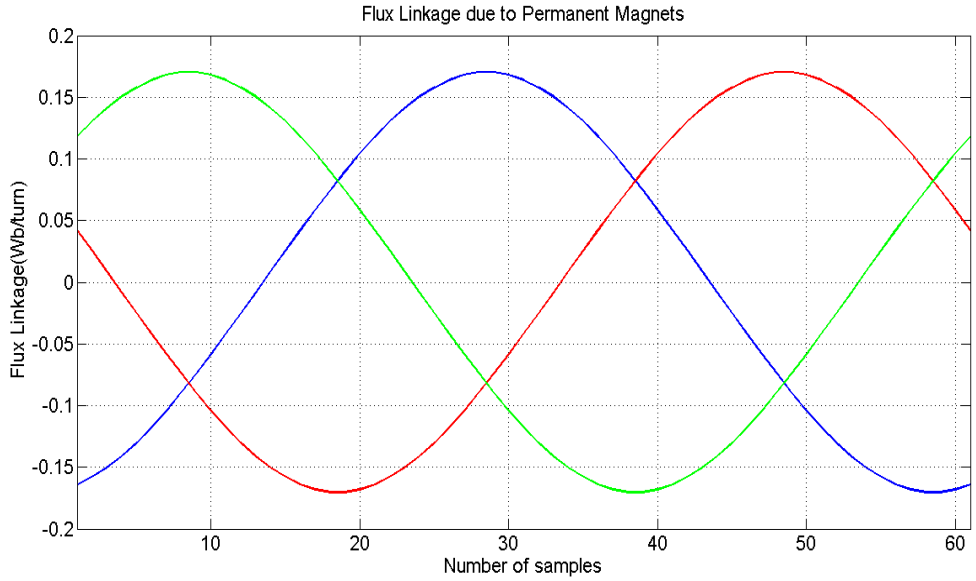

Figure 4-3: Flux Linkage due to Permanent Magnets

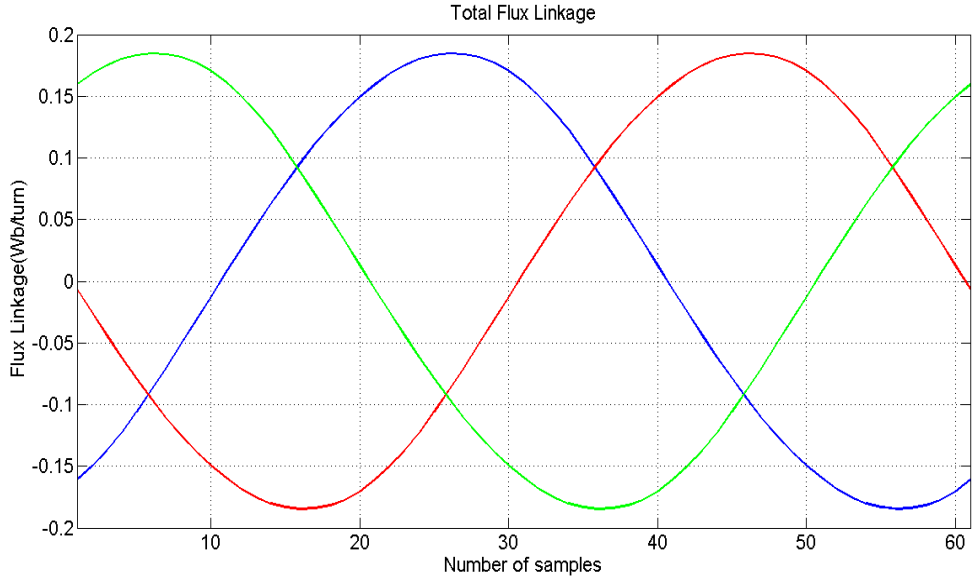

Figure 4-4: Total Flux Linkage

All the simulations performed in order to obtain previous and following graphs

have been done for an electrical revolution. Total flux linkage obtained by setting the current sources to the current supply value may bee seen in figure 4-4. It presents a maximum value of 0.1845 Wb/turn and thus the value for the flux linkage produced by effect of the currents circulating through the windings is 0.0143 Wb/turn, quite small if compared with the total, accounting only for 7.75% of it.

For all figures shown previously and in following sections, the number of samples seen on axis X corresponds also to the time in milliseconds, thus each millisecond, a new sample is taken. The total number of samples (60) corresponds to one electrical revolution which has been calculated employing the generator frequency seen on expressions 4.2 and 4.3.

$$f = \omega_m p \tag{4.2}$$

Where ω_m is the mechanical speed in rad/s and p is the number of pole pairs.

$$f = \frac{\omega_{rpm} poles}{60 \cdot 2} = \frac{100 \cdot 20}{120} = 16.67 Hz \tag{4.3}$$

Once the electrical frequency is known, the total number of milliseconds that must be simulated is obtained dividing one second or a thousand milliseconds by the frequency, this is, calculating the period.

$$T = \frac{1000}{16.67} = 60 ms \tag{4.4}$$

Choosing a total number of sixty time steps, each time step will last a millisecond and thus sixty samples will be taken.

4.3 Back EMF

Back electromotive force refers to the force produced in a rotating electric machine by the voltage. That voltage is proportional to the magnetic field, the number of turns of the windings and the speed of the motor.

Similar to what was done for flux linkage, the best way to obtain the back EMF

is to perform a no-load test and look at the voltage results. This has been done and displayed in figure 4-5. The maximum value obtained is 16.94V for all three

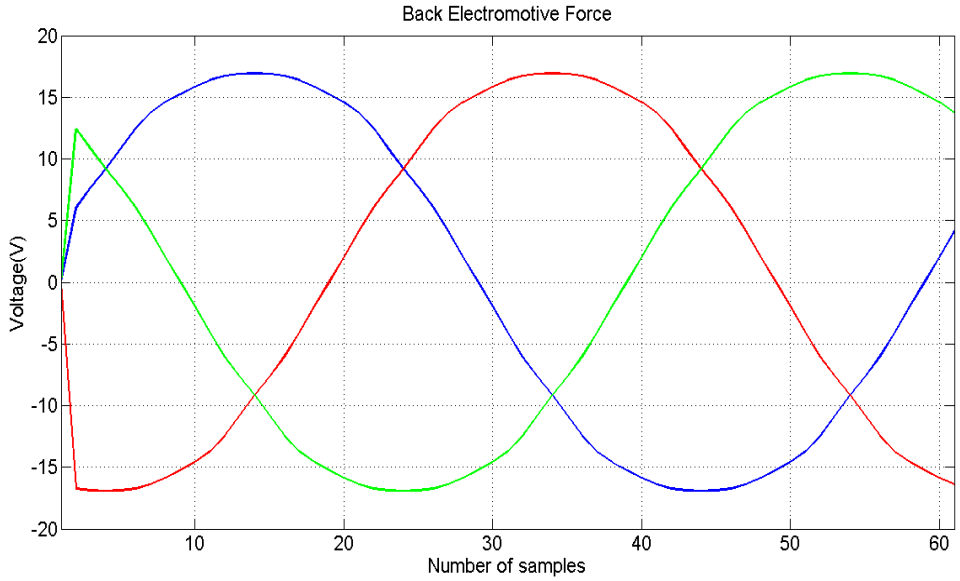

Figure 4-5: Back Electromotive Force

phases. The maximum voltage value obtained if simulating a load test is 21.12V. The reason why a no load test will point out the value of the back EMF can be explained with expression 4.3, which shows the different components of which the voltage is constituted.

$$V = RI + L\left(\frac{dI}{dt}\right) + m_L\left(\frac{dI}{dt}\right) + EMF \tag{4.5}$$

Where L is the inductance of the windings and m_L is the mutual inductance. Thus if current is set to 0A, the only component for the voltage will be the EMF and then the software employed will provide the previous results [3].

4.4 Torque

4.4.1 Average torque

Average torque can be calculated employing the results provided by MagNet through simulation. In figure 4-6 torque has been displayed with a maximum value of 19.13Nm

and a minimum of 18.86Nm.

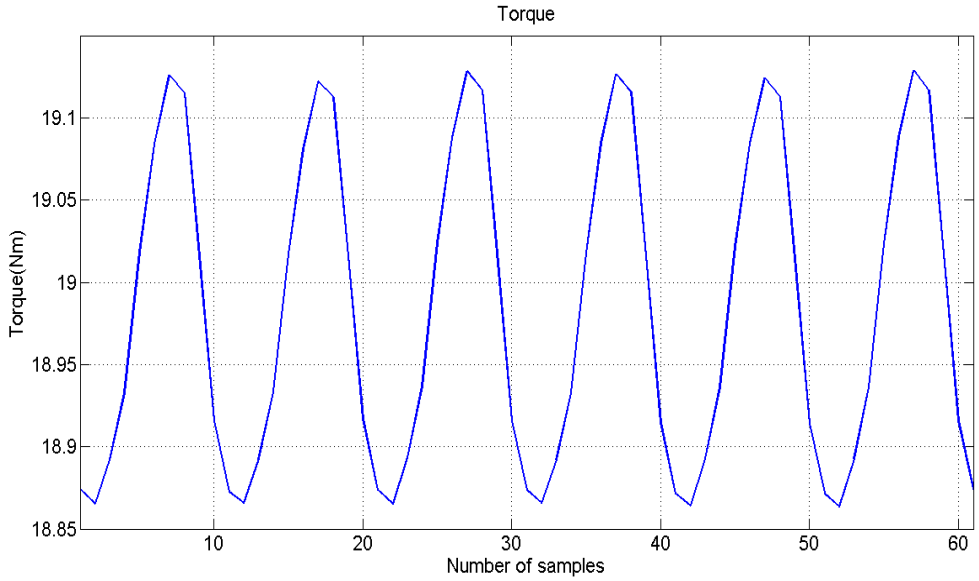

Figure 4-6: Torque

From the data that form 4-6 it is possible to obtain that the average Torque value is 18.9826Nm.

4.4.2 Cogging torque

Cogging torque is the torque produced due to the interaction between the magnets flux and the stator slots of a permanent magnet machine. It is a non-desired position dependent component of the torque which is especially prejudicial at low speeds. The task of analytical calculation and minimization of the cogging torque in PM machines is typically accomplished using Maxwell stress tensor methods [5].

The way to obtain it through MagNet simulation is by performing a no-load test which allows looking at the torque produced by the configuration of the machine, this is, the inherent torque of the device without taken into consideration supply current or any other variable.

Figure 4-7 shows the graph for the cogging torque provided by MagNet where it is possible to see that the values oscillate around zero from a minimum of -0.015Nm to a maximum of 0.01Nm.

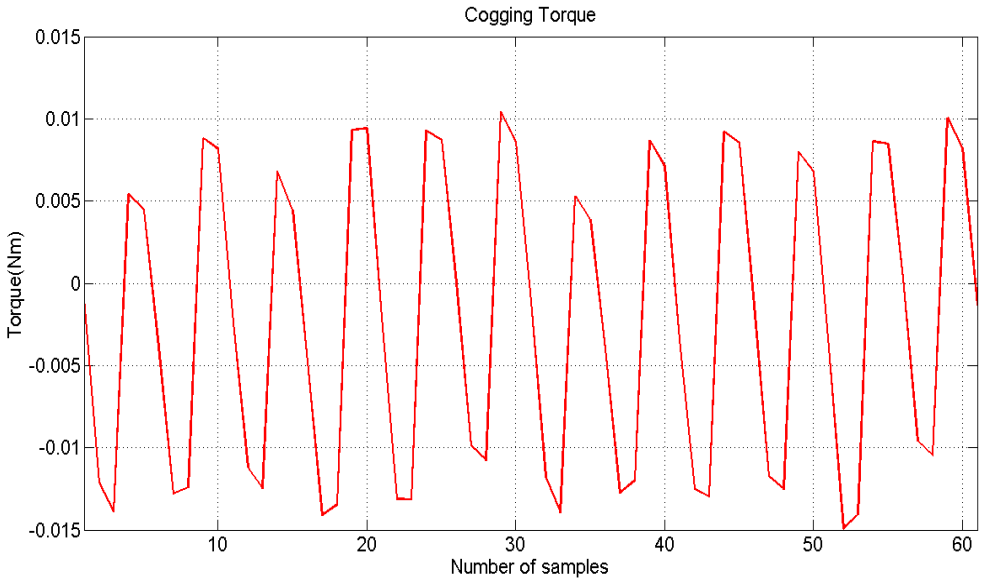

Figure 4-7: Cogging Torque

4.4.3 Torque ripple

Torque ripple is the periodic increase or decrease in output torque during the rotation of an electric machine usually expressed as a percentage of the total.

Among the possible sources of torque ripple, the main ones are the difference in amplitude in phase back-EMF or currents, the phase offset deviation between phases and the presence of harmonic components.

For the first case, and considering the amplitude of the back-EMF or the current in phase A to be a factor of (1+Δ) greater than ideal, the torque will be as seen on expression 4.4.3 and 4.4.3.

$$T(\theta) = K_p I_p[(1+\Delta)cos^2(\theta) + cos^2(\theta - \theta_{ph}) + cos^2(\theta + \theta_{ph})] \tag{4.6}$$

$$T(\theta) = \frac{3+\Delta}{2} K_p I_p + \frac{\Delta}{2} K_p I_p cos(2\theta) \tag{4.7}$$

Then, as the constant torque produced has increased to (3+Δ) $K_p I_p/2$ and a torque ripple term at the second harmonic of the fundamental electrical frequency appears with amplitude $\Delta K_p I_p/2$, the ratio of the amplitude of the torque ripple to the

constant torque produced is:

$$\frac{\Delta}{3+\Delta} \approx \frac{\Delta}{3} \tag{4.8}$$

Using this approximation a 3% amplitude error in one phase produces a peak torque ripple of approximately 1% [3]. If looking at the second source of torque stated at the beginning of this section, when the phase offset of a back-EMF or current shape deviates from the ideal, it is possible to obtain that a mere 0.03rad($\approx 1.72°$) phase misalignment produces 1% peak torque ripple. The third possibility is not easily obtained as it is subject to harmonic content.

For the case under study and going back to the results obtained from $MagNet$, torque ripple can be easily spotted on figure 4-6 previously shown. The difference between the lower and the upper peaks is 0.2651Nm which represents approximately 1.4% of the total.

4.5 Current density

In electromagnetism current density is defined as the electric current per cross sectional unit area and usually displayed as "J". It is defined as a vector whose magnitude is the electric current per cross-sectional area at a given point in space. In SI units, the electric current density is measured in amperes per square meter but usually employed as amperes per square millimeter.

Current density together with the electrical loading plays a crucial role in the thermal criterion and calculation of the temperature rise during operation of electrical machines. For naturally cooled machines like the case under study the typical value for current density is around $4\text{A}/mm^2$. A common expression to define current density is the one that relates it to the electrical loading "A", the slot area "A_{slot}", the slot-fill factor "F_{slot}" and the slot pitch "λ". It has been shown in expression (4.5). This equation can be also related to the slot-depth "d" and the tooth width "t" [6].

$$J = \frac{A\lambda}{F_{slot}A_{slot}} = \frac{A}{F_{slot}d(1-\tau)} \tag{4.9}$$

Where τ=t/λ, and A is described by expression 4.5.

$$A = \frac{2mN_{ph}I_{rms}}{\pi D} \tag{4.10}$$

Where m is the number of phases, N_{ph} is number of turns per phase, I_{rms} is the supply current effective value and D is the stator outer diameter. Substituting everything on the previous expression leads to solved equation 4.5.

$$A = \frac{2 \cdot 3 \cdot 320 \cdot 8/\sqrt{2}}{\pi \cdot 155 \cdot 10^{-}3} = 22.3 \cdot 10^{3} \tag{4.11}$$

Once the current loading is known, it is possible to go back to expression 4.5, substitute all values and obtain the current density analytical value seen in 4.5.

$$J = \frac{22.3 \cdot 10^{3}}{0.5 \cdot 23\left(1 - \frac{6.48}{12.43}\right)} = 4.05 A/mm^{2} \tag{4.12}$$

Obtaining a value very close to 4A/mm^2 which as it was said before is in the common range for this kind of machines.

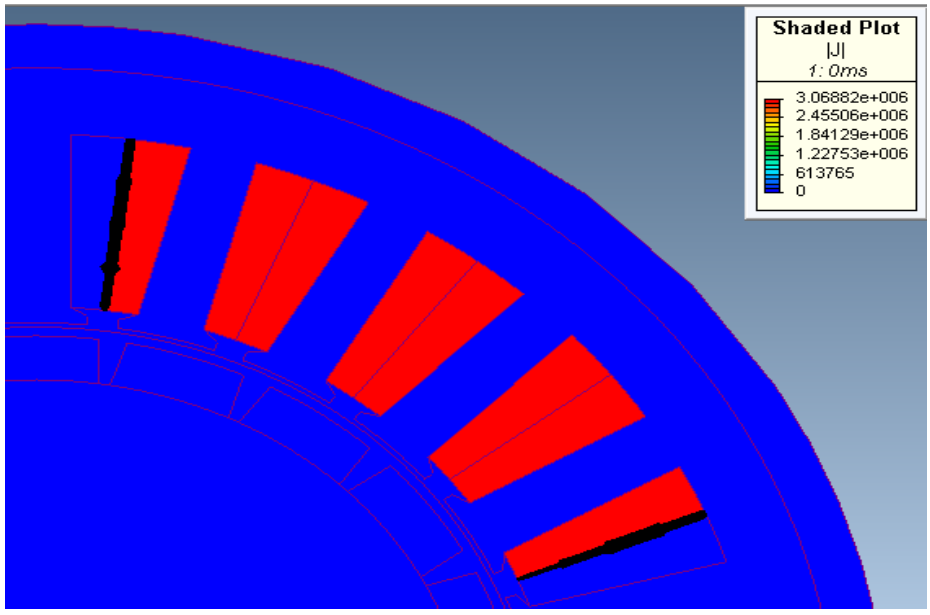

Figure 4-8: Current Density

The way to obtain the value through *MagNet* operation is rather easy. It consist

on measuring the value for the current density in the point of operation where the waveform of the current supply is at 90 degrees which corresponds to the time instant at 15 milliseconds and then multiplying that value by two and dividing it by π. Finally, as $MagNet$ wasn't taking into account the winding factor which is 50%, it is necessary to multiply the final value by two again.

If looking at figure 4-8, it is possible to see that the value is 3.0688A/mm^2. Then following the process previously described it is possible to obtain a value of 3.9073A/mm^2 which is not far from the one calculated analytically.

4.6 Copper Losses

Copper loss refers to the wasted energy in form of heat produced by electrical currents in conductors. The term is applied regardless of whether the windings are made of copper or another conductor, such as aluminum. The term load loss is closely related but not identical, since an unloaded transformer will have some winding loss.

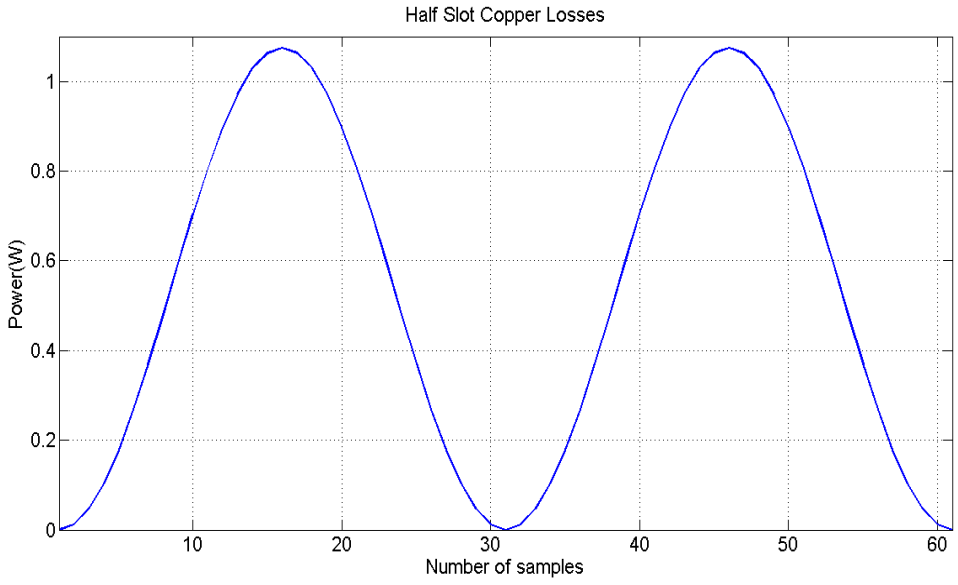

Figure 4-9: Half Slot Copper Losses

Regarding copper losses, the obtainment of results from $MagNet$ is an automatic process as they are among the values provided right after simulating. The value of

ohmic losses for a single layer of slot (double layer side-by-side windings) may be seen in graphical form in figure 4-9.

From the values shown in figure 4-9 it is possible to obtain the total average value of copper losses by obtaining the average of those values employed to draw the curve, multiply it by two to obtain the losses of each slot and then multiply it by twenty-four to obtain the total value which in the case under study is 25.3769W.

It is also possible to obtain copper or ohmic losses through analytical expressions which on its simplest form are described as it was seen on model optimization and also in equation 4.6.

$$P_{copper} = RI^2 \tag{4.13}$$

The problem is that obtaining the resistance value depends on a far more complicated expression seen on 4.6.

$$R = \frac{2\rho_{cu} L N_{ph} I_{rms}^2}{(pq) A_{slot} F_{slot}} \tag{4.14}$$

Where ρ_{cu} stands for electrical resistivity of copper, $L = (P_a + P_{sl})N_{ph}^2$ been P_a the air-gap permeance and P_{sl} the slot leakage permeance, N_{ph} is the number of turns per phase, I_{rms}^2 is the effective value of the current supply, p is the number of pole pairs, $q = N_s/(m \cdot 2p)$ been N_s the number of slots and m total number of phases, A_{slot} is the slot area and F_{slot} is the slot-fill factor.

In short, it is not worth using the equation as it would be necessary to take some characteristics from the software model due to the absence of a more complex analytical model.

4.7 Iron Losses

Iron losses also known as core losses are a result of the effect produced by the varying magnetic field induced by the alternating current passing through the windings on the core which makes some of the power dissipate as heat or noise. There are mainly two processes involved in this loss, hysteresis and eddy currents.

Analytically, iron losses can be obtained employing the expression known as Steinmetz's loss which has been displayed in 4.7. It is formed by two components, the first one due to hysteresis and the second one due to eddy current losses. It provides values in W/kg.

$$P_{iron} = k_h f^{\alpha} B^{\beta} + k_e (sfB)^2 \tag{4.15}$$

Where k_h and k_e are the hysteresis and eddy current constants, f is the current supply frequency, B is the peak flux density, and s is the lamination thickness ratio. All these values are provided and employed by $MagNet$ for each material present on the software [7].

In practice it is not necessary to look for these values as iron losses for both stator yoke and rotor core are provided by $MagNet$ automatic simulation results in time averaged form separated into hysteresis and eddy current losses.

4.7.1 Hysteresis

The varying magnetic field through the core changes the magnetization of its material producing a process of expansion and contraction which causes losses in form of heat. This process known as hysteresis loss can be seen in the material B-H loop.

For the case under study stator yoke hysteresis losses are 1.2629W while for the rotor core are 1.2702mW.

4.7.2 Eddy Current

Eddy currents losses are a result of the electric resistance of the core material to the circulating currents produced by the varying magnetic fields. That resistance dissipates part of the power in form of heat. The power loss is proportional to the area of the loops and inversely proportional to the resistivity of the core material [8].

For the final chosen model, eddy current losses are 49.6397mW for the stator and 0.0284mW for the rotor. It is possible to affirm that both values from eddy current losses and in general, values from rotor iron losses are negligible when compared to stator yoke hysteresis losses.

Magnets

Losses in the magnets are caused by eddy-currents which as it was briefly explained before are due to the variation of flux-density in the magnets. The process is exactly the same as the generation of eddy-currents in general.

With respect to eddy currents in the magnets a way to calculate it is by looking at the ohmic losses in the magnets provided by MagNet. Looking at the values from the 20 poles seen in figure 4-10 it is possible to affirm that the average losses for this specific element are around 0.58mW. The maximum value reached among all the data collected was 1.44mW. It is easy to see that figure 4-10 represents two magnets

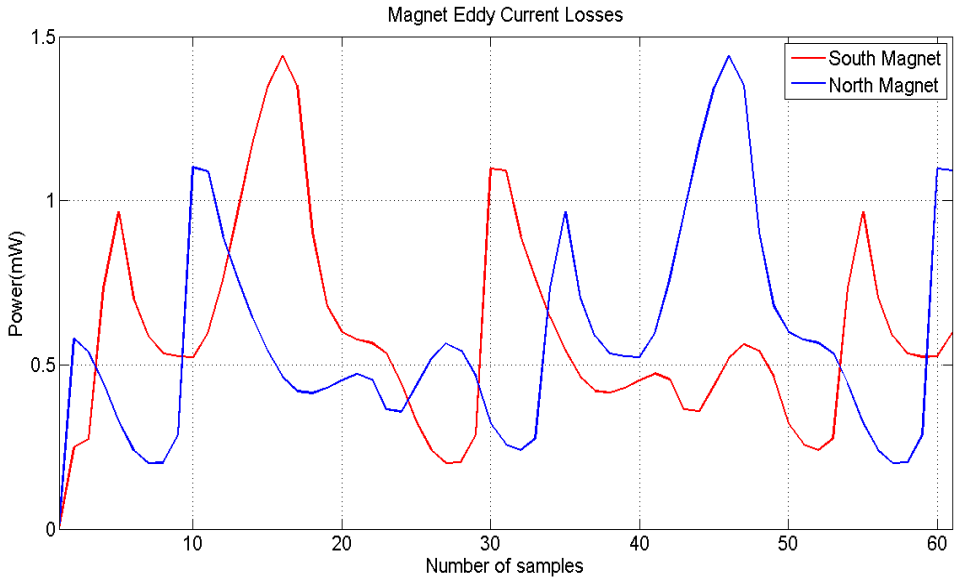

Figure 4-10: Magnet Eddy Current Losses

that for being immediately close to each other are shifted 90 degrees, in other words, one pole is facing one direction and the next one is facing the opposite in order to achieve that varying magnetic field responsible for the generation of electricity in the windings.

Sleeve

Mainly produced by the higher space harmonics due to slot openings; however, in the case of full-pitch stator winding, other space harmonics can also be significant.

Regarding the sleeve eddy current losses, for the case under study the sleeve material considered was air then they were not eddy currents involved in this part of the machine. For a more realistic application the sleeve material should be changed to carbon fiber for instance and new simulations should be carried out in order to obtain values from the model.

4.8 Demagnetization and variation with temperature

The study of demagnetization in a permanent magnet motor or generator can be done by looking at how two variables change according to a temperature difference. Those variables, explained below, are remanent flux density and coercivity.

4.8.1 Remanent flux density

Been "B_r" the remanent flux-density, its demagnetization is specified in terms of "α_{B_r}" which stands for reversible temperature coefficient of "B_r" expressed in percentage per Celsius degree.

$$B_r(t^\circ) = B_r(20^\circ C)\left[1 + \alpha_{B_r}\frac{t^\circ - 20}{100}\right] \tag{4.16}$$

Where $B_r(20^\circ\text{C})$ is 1.1T, the value of B_r at 20°C, usual value for room temperature. The coefficient $alpha_{B_r}$ is around -0.09 -0.15%/°C in the case of neodymium iron boron magnets. In order to try this behavior a temperature of 60°C is chosen as maximum machine temperature under operation to observe the demagnetization:

$$B_r(t^\circ) = 1.1\left[1 - 0.12\frac{60 - 20}{100}\right] = 1.0472T \tag{4.17}$$

It is possible to see that the remanent flux-density does not vary significantly for that temperature difference giving this material good behavior when referring to "B_r".

4.8.2 Coercivity

Coercivity (H_c) is a measure of a ferromagnetic or ferroelectric material to withstand an external magnetic or electric field. For ferromagnetic material the coercivity is the intensity of the applied magnetic field required to reduce the magnetization of that material to zero after the magnetization of the sample has been driven to saturation. Thus coercivity measures the resistance of a ferromagnetic material to becoming demagnetized.

When referring to "H_c" the temperature coefficient is between -0.4 and -0.8 "%"/°C [9]. This will cause a significant change in coercivity during operation.

$$H_c(t^\circ) = H_c(20^\circ C)\left[1 + \alpha_{H_c}\frac{t^\circ - 20}{100}\right] \tag{4.18}$$

The coercivity of neodymium iron boron magnets at room temperature according to $MagNet$ is 827.6kA/m. Then the value obtained for the same temperature used before can be seen in expression (4.8.2).

$$H_c(t^\circ) = 827.6 \cdot 10^3\left[1 - 0.6\frac{60 - 20}{100}\right] = 628.98kA/m \tag{4.19}$$

As it was said before, the coercivity of neodymium iron boron magnets varies in a much greater way than the remanent flux density.

4.9 Radial forces

Permanent magnet machines are subject to great sources of vibration forces been them mainly radial forces and unbalanced magnetic forces. Taking into account the existence of rotor eccentricity, these forces are increased due to mechanical and magnetic coupling effects [10].

Regarding radial force, it is possible to obtain it in an oversimplified way as the product of the previously obtained torque multiplied by the velocity or linear speed. Knowing that the angular speed is 100rpm or 10.47rad/s and the rotor outer diameter

is 95mm, it is possible to obtain it as v $=\omega \cdot$r , and then the linear speed is equal to 0.99m/s.

Once the linear speed is known and assuming it is constant, the radial force may be calculated with the 60 measurements (or sample points) of motion rotor torque provided by $MagNet$.

The average force obtained from the total number of measurements is 18.79N. It is not displayed here as it looks exactly like the torque graphical representation shown in figure 4-6 with every value multiplied by 0.99.

Chapter 5

Conclusion

The market for electric bicycles is seeing a boom which has not seen on its history before and that is why through constant innovation it will be allowed to increase and maintain the interest of users promoting the use of these vehicles and thus contributing positively to an improvement of the environment as well as people's quality of life.

It is possible to state firmly that the project objectives have been completely fulfilled, as it has provided a final model of electric generator that complies with design constraints, that will be manufactured in the near future and used as first prototype in a much larger project consisting on creating the chain-less electric bicycle described in the introduction.

Final characteristics achieved through model optimization and further analysis satisfy well enough design constraints, these and the results have been summarize in tables 5.1 and 5.2 respectively.

5.1 Future Work

The final model provided by this project accounts for the first prototype of generator which will be used as a start point for further improvement and for intensive testing previous to its implementation on a market product. As it was said on the introduction, this project is included within a much larger one that will comprise a whole electric bicycle, therefore and in this sense, there is still a large backlog in regard to

Variable	Value	Unit of Measurement
Slot/Pole Configuration	24/20	-
Number of Turns	40	-
Supply Current	8	Ampere
Tooth Width Ratio	0.6	-
Magnet Thickness	5	Millimeter
Magnet Angle	16.5	Degree
Slot Wedge Angle	20	Degree
Back Iron Thickness	7.5	Millimeter
Slot Opening	3	Millimeter
Tooth Tip Height	1	Millimiter

Table 5.1: Final Model Characteristics

Variable	Value	Unit of Measurement
Efficiency	88.1625	Percentage
Average Torque	18.9826	Newton Meter
Phase Peak Voltage	21.1201	Volt
Phase Flux Linkage	0.18453	Weber/Turn
Output Power	198.7848	Watt
Copper Losses	25.3769	Watt
Iron Losses	1.3138	Watt

Table 5.2: Final Model Results

the entire system. As the scope of this project only affects the generator, it will be in future works by new authors that these improvements and testing will take place.

Bibliography

[1] S.E.Skaar, Ø. Krøvel, R. Nilssen, "Distribution, coil-span and winding factors for PM machines with concentrated windings".

[2] A.E. Fitzgerald, Charles Kingsley, Jr., Stephen D. Umans, "Electric Machinery, Sixth Edition", New York, 2003.

[3] Dr. Duane Hanselman, "Brushless Permanent Magnet Motor Design, Second Edition", Electrical and Computer Engineering, University of Maine, Orono, USA, 2006.

[4] Stanely Humphries, "Tutorial: Surface integral expressions for electric/magnetic force and torque", Field Precision, 2012.

[5] Ayman M. El-Refaie, Thomas M. Jahns, Donald W. Novotny, "Analysis of Surface Permanent Magnet Machines with Fractional-Slot Concentrated Windings", IEEE Transactions on energy conversion, vol. 21, no. 1, March 2006.

[6] TJE Miller, "SPEED's Electric Machines", University of Glasgow, Department of Electronics and Electrical Engineering, 2002-2011.

[7] Jacek F. Gieras, Andreas C. Koenig, Laurence D. Vanek, "Calculation of Eddy Current Losses in Conductive Sleeves of Synchronous Machines", Proceedings of the 2008 International Conference on Electrical Machines.

[8] H. Polinder, M.J. Hoeijmakers, M. Scuotto, "Eddy-Current Losses in the Solid Back-Iron of PM Machines for different Concentrated Fractional Pitch Windings", Electrical Power Processing, Delft University of Technology, The Netherlands, 2007.

[9] Jacek F. Gieras, Rong-Jie Wang, Maarten J. Kamper, "Axial Flux Permanent Magnet Brushless Machines, 2nd Edition", 2008.

[10] Kyung-Tae K., Kwang-Suk K., Sang-Moon H., Tae-Jong K., Yoong-Ho J., "Comparison of Magnetic Forces for IPM and SPM Motor with Rotor Eccentricity", IEEE Transactions on magnetics, vol. 37, no. 5, September 2001.